ORIGINAL RESEARCH ARTICLE

Oxidation Mechanism of Vanadium Slag with High MgO Content at High Temperature

JIANG DIAO, LIANG LIU, JING LEI, WEN-FENG TAN, HONG-YI LI, and BING XIE

Based on two considerations of making full use of the residual heat of vanadium slag and exploring a novel green vanadium extraction process, this article employs vanadium slag with high MgO content as raw material, blowing oxygen into the molten vanadium slag and using the residual heat of the vanadium slag to carry out high-temperature roasting experiments. XRD and SEM/EDS were used to characterize the phase evolution and morphology of vanadium slag with high MgO content during oxidation. The results show that at a high temperature of 1723 K, the trivalent vanadium in vanadium slag can be partly transformed into acid-soluble pentavalent vanadium. Titanium-bearing spinel was oxidized into a large amount of strip pseudobrookite Fe_2TiO_5. After oxidation, vanadium existed in the form of the solid solution of magnesium pyrovanadate $(Mg, Mn, Ca)_2V_2O_7$. The leaching rate of roasted vanadium slag with high MgO content is significantly higher than that of industrial vanadium slag. With the increase of oxygen blowing time from 10 to 30 minutes, the leaching rate of roasted vanadium slag with high MgO content increases from 23.19 to 53.69 pct.

https://doi.org/10.1007/s11663-020-02000-w

I. INTRODUCTION

VANADIUM is an important metal, which is widely used as a steel alloy additive, catalyst in the chemical industry and electrode material in the automobile battery, *etc*.[1] Vanadium–titanium magnetite ore is the main raw material for vanadium extraction. About 88 pct of vanadium worldwide is extracted from vanadium-titanium magnetite ore.[2,3] The route of extracting vanadium from vanadium-titanium magnetite ore is to convert the ore into vanadium-bearing hot metal through blast furnace or other ironmaking processes and then blow oxygen into the converter to enrich vanadium in the hot metal into slag phase. The vanadium slag obtained is used as the subsequent raw material for vanadium extraction, and vanadium is extracted through pretreatment, roasting, leaching and other processes.[4–6]

Vanadium slag is a typical complex system with multiple oxides, in which vanadium exists in the form of vanadium spinels wrapped with olivine and other silicates. Apart from the hindrance caused by the silicates, the vanadium spinels are so sufficiently stable that it is impossible to directly leach vanadium into liquid for extracting vanadium.[7,8] A well-known and traditional process of roasting-leaching operations was introduced to recover vanadium from vanadium slag. The roasting-leaching operation requires mechanical crushing and high-temperature alkali roasting to destroy the outer package of the spinel and promote the oxidation of the low-valent vanadium (III) in the spinel to high-valent vanadate (V).[9]

According to different roasting additives, the industrialized vanadium extraction methods can be divided into the sodium method and calcification method.[10] The additives used in the sodium method are NaCl, Na_2SO_4, Na_2CO_3, *etc*.[11,12] Low-valent vanadium in spinels is oxidized by oxygen to the maximal extent and transforms into water-soluble sodium vanadates in the presence of sodium salts at 973 to 1123 K. Subsequently, ammonium sulfate is added to the sodium vanadate solution to precipitate ammonium vanadates, which can be calcinated to yield V_2O_5. The low-melting sodium salt produced during the roasting process will cause material sticking and hinder the continued oxidation of vanadium. Harmful gases such as SO_2, SO_3, Cl_2, and HCl will be generated during the roasting process, which will corrode the equipment and pollute the environment.[13,14] The tailings and wastewater after vanadium

JIANG DIAO, LIANG LIU, JING LEI, WEN-FENG TAN, HONG-YI LI and BING XIE are with the College of Materials Science and Engineering, Chongqing University, Chongqing 400044, P.R. China and also with the Chongqing Key Laboratory of Vanadium-Titanium Metallurgy and Advanced Materials, Chongqing University, Chongqing 400044, P.R. China. Contact e-mail: diaojiang@163.com

Manuscript submitted July 22, 2020. Accepted October 4, 2020.
Article published online January 4, 2021.

extraction contain large amounts of Na^+ and cannot be recycled in the steel production process.[15] Due to the environmental pollution caused by sodium roasting, an environmentally friendly new technology of vanadium extraction by calcification roasting has attracted more attention. The calcification method is roasted with CaO or $CaCO_3$ at 1073 K to 1473 K to produce calcium vanadate, which can be leached by acid. During the acid leaching process, the precipitation of $CaSO_4$ could inhibit the dissolution of vanadates, thus reducing the leaching ratio of vanadium.[16,17] Moreover, Due to the large amount of $CaSO_4$ in the tailings of vanadium extraction, it is difficult to use economically and can only be discarded. Thus, it can be seen that vanadium slag roasting additives bring serious problems to the disposal of solid waste, waste water and waste gas. To solve the pollution problems caused by the roasting agent, Li *et al.*[18] used MgO to replace the existing sodium and calcium salts to achieve the conversion of spinel to soluble magnesium vanadates. The recovery of valuable metal ions from wastewater and the recycling of the roasting agent MgO are realized through process design. In addition, the vanadium tailings can be returned to the blast furnace to recover iron and vanadium resources.

Another problem in the current vanadium extraction process is that the sensible heat of vanadium slag is not utilized. The temperature of vanadium slag discharged from the converter is about 1573 K, and it needs to be cooled to room temperature for crushing, milling, mixing, magnetic separation and iron removal and then heated to 973 K to 1473 K for roasting, so that the heat energy of vanadium slag is completely wasted. Song *et al.*[19–21] studied the addition of Na_2CO_3/CaO and oxygen to molten vanadium slag, using the heat energy of vanadium slag for direct roasting. The effect of alkali salt content on the oxidation of vanadium slag was analyzed, but the phase transformation of spinel in the oxidation process was not discussed in depth.

In this article, MgO is used as a roasting additive, and the heat energy of vanadium slag is directly used for roasting treatment. Under the high temperature at 1723 K, the low-valent vanadium in the molten vanadium slag is transformed into high-valent vanadium to shorten the extraction time of vanadium and save energy. By comparing the phases of vanadium slag with high MgO content and industrial vanadium slag, the existing forms of magnesium and vanadium in the slag are analyzed. The phase evolution and morphology of vanadium slag with high MgO content during oxidation are also discussed.

II. EXPERIMENT SECTION

A. *Materials*

The chemical composition of the industrial vanadium slag used in the experiments was analyzed by X-ray fluorescence spectroscopy (XRF, SHIMADZU LAB CENTER XRF-1800) and listed in Table I. The MgO roasting additive was dried in an oven at 378 K for 12 hours prior to use. To obtain vanadium slag with high MgO content, 5 wt pct MgO was added into the molten industrial vanadium slag.

Table I. Chemical Composition of Vanadium Slag, Wt Pct

FeO	V_2O_3	SiO_2	TiO_2	MnO	MgO	Al_2O_3	CaO
38.53	15.37	13.51	12.60	9.47	4.01	3.47	3.02

B. *Methods*

A 50 g dried industrial vanadium slag was added into a corundum crucible and melted at 1723 K. After full melting, MgO was added and quickly stirred evenly. A double-hole alumina pipe with an inner diameter of 1 mm was inserted into the molten vanadium slag. Then, oxygen gas was blown into the molten slag. The oxygen flow rate and oxygen blowing time were 3 to 10 L/min and 0 to 30 minutes, respectively. After oxygen blowing, the crucible was taken out from the furnace, cooled in air to room temperature, and then ground into powder with particle size < 74 μm.

An X-ray diffractometer (XRD, Rigaku D/max 2500 PC) was used to characterize the phase in the powder sample. Morphology and element distribution in bulk samples were detected by a scanning electron microscope (SEM, TESCAN VEGA III) equipped with an energy disperse X-ray spectroscopy (EDS, INCA Energy 350). The oxidation effect of vanadium slag was expressed by the leaching rate of vanadium. The elemental vanadium concentrations in the leaching liquor were determined *via* an inductively coupled plasma-atomic emission spectrometer (ICP-AES, Thermo Fisher Scientific iCAP 6300 Duo) with the limit of determination of 0.001 mg/L. The thermodynamic calculations were performed using the FactSage 6.3 software.

III. RESULTS AND DISCUSSION

A. *Existing Forms of Mg and V in Vanadium Slag with High MgO Content*

Figure 1 shows the XRD patterns of industrial vanadium slag and vanadium slag with high MgO content. The main phases of industrial vanadium slag are spinel phase (Fe, Mg)V_2O_4, (Mg, Fe)$_2TiO_4$ and olivine phase Fe_2SiO_4. V is concentrated in spinel phase, and Mg distributes in each phase. With the increase of MgO content in vanadium slag, part of Fe^{2+} (ion radius 0.74 Å) in Fe_2SiO_4 is replaced by Mg^{2+} (ion radius 0.66 Å) with a smaller ion radius, which leads to smaller cell parameters and an overall right shift of the XRD peak.[22] Therefore, the three strong peaks of olivine phase (2θ = 25.07, 31.65 and 51.34 deg) in vanadium slag with high MgO content shift 0.25, 0.35 and 0.39 deg to high angles, respectively.

The SEM images and EDS results of the vanadium slag with high MgO content are shown in Figure 2 and Table II, respectively. No independent MgO was detected, which is consistent with the XRD results, indicating that the additional MgO has completely entered the vanadium slag phase. Figure 2 shows the vanadium slag with high MgO content is composed of three kinds of mineral phases, *i.e.*, bright-white spinel phase, gray-white olivine phase and gray-black silicate matrix. Mg is concentrated in the olivine phase and spinel phase, and a small amount distributes in the silicate matrix. V is only concentrated in the spinel phase; the content is about 17 at pct.

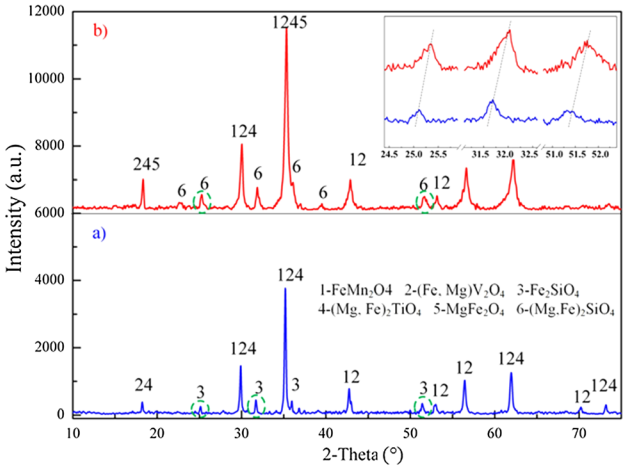

Fig. 1—XRD pattern of the samples: (*a*) industrial vanadium slag; (*b*) vanadium slag with high MgO content.

B. *Phase Evolution of Vanadium Slag with High MgO Content During Oxidation*

Figure 3 shows the XRD pattern of vanadium slag with high MgO content after blowing oxygen for different times. After blowing oxygen for 1 minute, the peaks of olivine phase $(Mg, Fe)_2SiO_4$ all disappeared, and the weak diffraction peaks of pyroxene phase $MgSiO_3$ appeared. The pseudobrookite Fe_2TiO_5 diffraction peak began to appear, accompanied by a weak magnesium pyrovanadate $Mg_2V_2O_7$ diffraction peak. This indicates that the olivine phase reacted completely after oxygen blowing for 1 minute, and part of the exposed spinel gradually began to oxidize. Figure 4 shows that the olivine phase in vanadium slag preferentially reacts with MgO in oxygen atmosphere. After blowing oxygen for 3 minutes, the peak intensity of the spinel phase diffraction peaks weakened significantly, and Fe_2O_3 diffraction peaks gradually began to appear. The diffraction peaks of $Mg_2V_2O_7$ and Fe_2TiO_5 gradually increased, and the peak shape became sharp, indicating that the content gradually increased. The

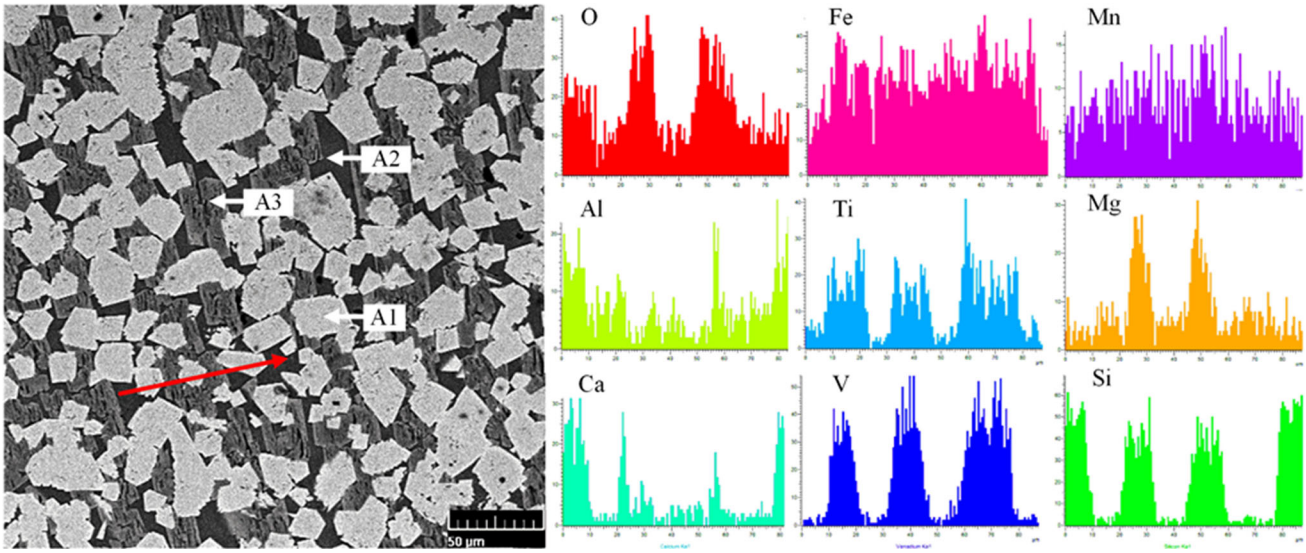

Fig. 2—SEM image of vanadium slag with high MgO content.

Table II. EDS Results of Vanadium Slag with High MgO Content, At Pct

	Mineral Phase	O	Mg	Al	V	Mn	Fe	Ti	Si	Ca
A1	spinel	43.17	7.67		17.93	4.02	18.92	8.29		
A2	silicate matrix	61.74	0.96	4.52		2.12	5.50	1.34	18.33	5.49
A3	olivine	56.89	10.77			4.26	13.16		14.93	

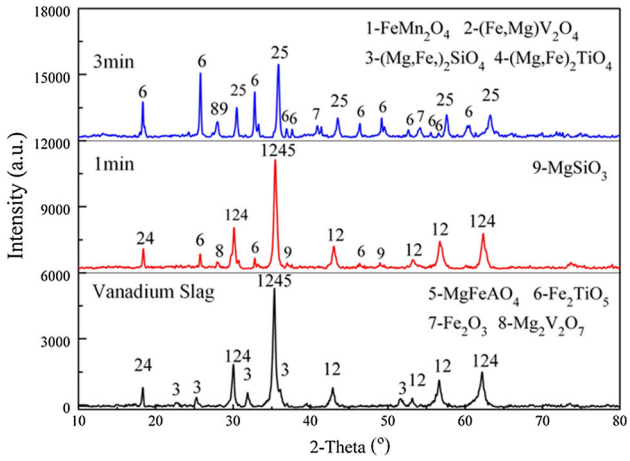

(a)

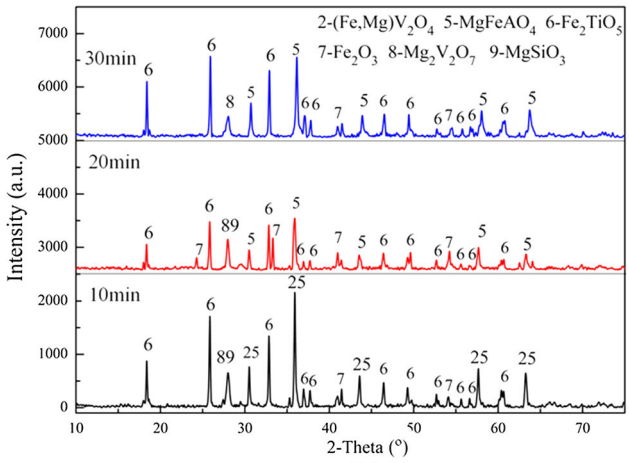

(b)

Fig. 3—XRD patterns of vanadium slag with high MgO content after different oxygen blowing times: (*a*) 0, 1, and 3 min, (*b*) 10, 20, and 30 min.

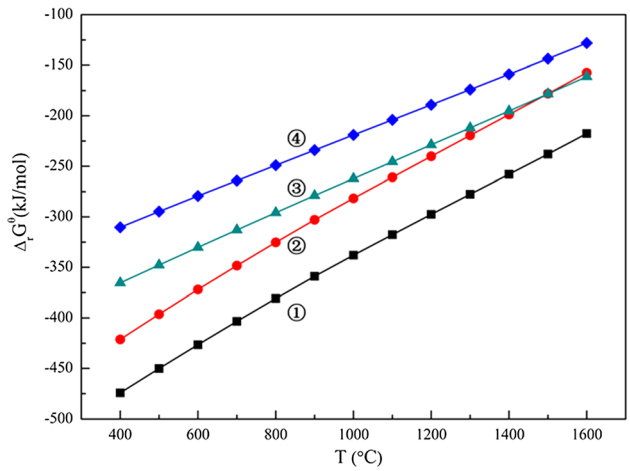

Fig. 4—Relationship of $\Delta_r G^\theta$ between the main phases of vanadium slag and MgO: ① $2Fe_2SiO_4 + 2MgO + O_2 = 2MgSiO_3 + 2Fe_2O_3$; ② $2Fe_2TiO_4 + MgO + O_2 = MgTi_2O_5 + 2Fe_2O_3$; ③ $8/5MgO + 4/5FeV_2O_4 + O_2 = 4/5Mg_2V_2O_7 + 2/5\ Fe_2O_3$; ④ $MgO + MgV_2O_4 + O_2 = Mg_2V_2O_7$.

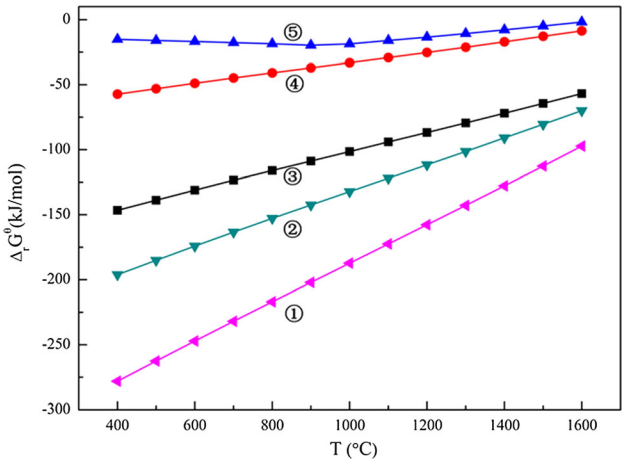

Fig. 5—Relationship of $\Delta_r G^\theta$ between $MgSiO_3$ and vanadium-containing phases: ① $MgSiO_3 + MgV_2O_4 + O_2 = Mg_2V_2O_7 + SiO_2$; ② $MgSiO_3 + 1/2FeV_2O_4 + 5/8O_2 = 1/2Mg_2V_2O_7 + 1/4Fe_2O_3 + SiO_2$; ③ $MgSiO_3 + 1/2V_2O_3 + 1/2O_2 = 1/2Mg_2V_2O_7 + SiO_2$; ④ $MgSiO_3 + VO_2 + 1/4O_2 = 1/2Mg_2V_2O_7 + SiO_2$; ⑤ $MgSiO_3 + 1/2V_2O_5 = 1/2Mg_2V_2O_7 + SiO_2$.

diffraction peak of the $MgSiO_3$ disappeared, and the thermodynamic calculation results in Figure 5 show that $MgSiO_3$ can continue to react as an intermediate phase. With the increase of oxygen blowing time, the diffraction peak intensity of spinel phase decreases continuously, while that of $Mg_2V_2O_7$ increases continuously. After blowing oxygen for 20 minutes, the intensity of the diffraction peak of $Mg_2V_2O_7$ remained unchanged. After the spinel phase was completely oxidized, it mainly includes Fe_2O_3, Fe_2TiO_5, $MgFeAlO_4$ and $Mg_2V_2O_7$. After blowing oxygen for 30 minutes, the intensity of the diffraction peak of the spinel phase increased slightly because of the spinel phase $MgFeAlO_4$ continuously generated during the spinel oxidation process.

C. *The Morphology of Vanadium Slag with High MgO Content During Oxidation*

Seen from Figure 6, after being oxidized for 3 minutes, the olivine crystals in roasted vanadium slag with high MgO content completely disappeared, the spinel phase was oxidized into a large amount of strip pseudobrookite Fe_2TiO_5, and vanadium gradually began to disperse in the silicate matrix. Mg is mainly concentrated in the spinel phase, and a small amount exists in the pseudobrookite and silicate matrix. V is mainly concentrated in the gray-black silicate matrix and pseudobrookite. The vanadium content in the silicate matrix is about 7.35 at pct, and the vanadium content in the pseudobrookite is about 2.52 at pct.

After being oxidized for 20 minutes, bright white Fe_2TiO_5 and spinel phases were embedded on the gray black matrix of vanadium slag. Some of the elongated crystals are blocked by spinel phase to form short rod-shaped pseudobrookite. Compared with oxygen blowing for 3 minutes, the V content in silicate matrix increases from 7.35 at pct to about 14 at pct. The content of V in pseudobrookite remains unchanged at 2

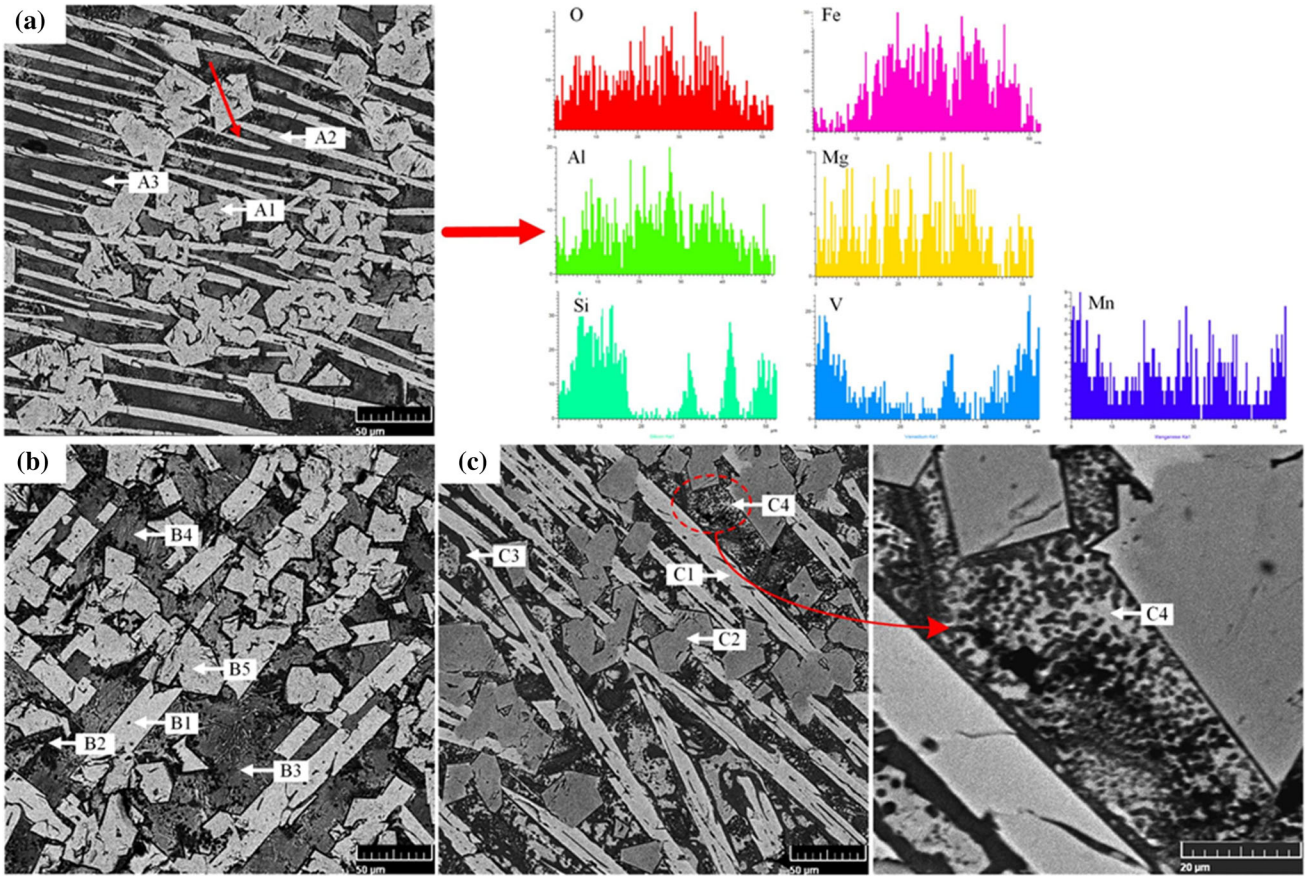

Fig. 6—SEM image of vanadium slag with high MgO content after different oxygen blowing times: (*a*) 3 min; (*b*) 20 min; (*c*) 30 min.

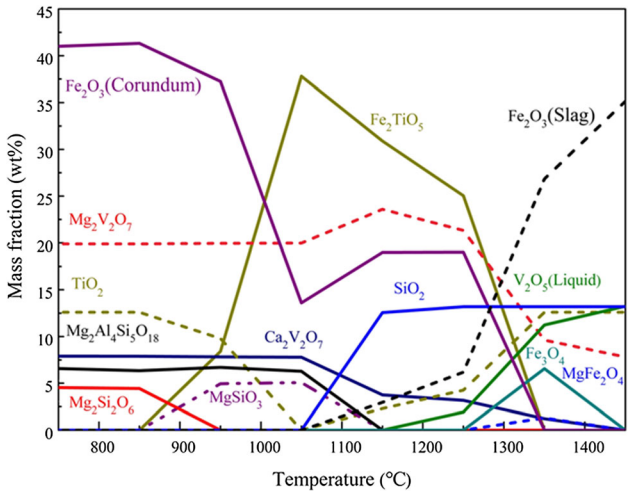

Fig. 7—Multiphase equilibrium of vanadium slag with high MgO content at different temperatures.

to 3 at pct. The Si content in the silicate matrix decreased from 19.99 to < 14 at pct. A large number of black dot-shaped silicon-rich phases accumulate around the spinel crystals, and the silicon content is as high as 26.18 at pct.

The multiphase equilibrium of vanadium slag with high MgO content at different temperatures calculated by FactSage is shown in Figure 7. Mg^{2+} in silicate matrix reacts with iron oxides in various ways to form $MgFe_2O_4$,[23–25] thereby generating free SiO_2. The presence of Al^{3+} introduced by an alumina crucible and Fe^{3+} undergo isomorphic substitution, resulting in the formation of $MgFeAlO_4$. The reaction is shown in Eqs. [1], [2].

$$2MgSiO_3 + 4FeO_X + (3 - 2X)O_2 \rightarrow 2MgFe_2O_4 + 2SiO_2 \ (x = 1 - 1.5) \quad [1]$$

$$2MgFe_2O_4 + l_2O_3 \rightarrow 2MgFeAlO_4 + Fe_2O_3 \quad [2]$$

As shown in Table III, after oxidation for 30 minutes, the crystal formed by the reaction grows and polymerizes, which makes the bright white pseudobrookite on the silicate matrix bulky. Compared with oxygen blowing for 20 minutes, the V content in the matrix decreases from 14.05 to 5.28 at pct. Amorphous morphology of the solid solution of magnesium pyrovanadate (Mg, Mn, Ca)$_2V_2O_7$ precipitated on the matrix, and the V content was as high as 20.21 at pct.

Table III. EDS Results of Roasted Vanadium Slag with High MgO Content, At Pct

Sample	No.	Mineral Phase	O	Mg	Al	V	Mn	Fe	Ti	Si	Ca
A	1	spinel	54.38	8.55	11.71	1.08	2.37	21.91			
	2	pseudobrookite	61.01	2.45	4.24	2.52		16.48	13.31		
	3	silicate matrix	59.46	2.37	3.54	7.35	3.86	1.6		19.99	1.83
B	1	pseudobrookite	56.07		4.65	2.75		21.17	15.36		
	2	silicon-rich phase	59.09	2.66	5.47	1.86	1.18	2.7		26.18	0.86
	3	silicate matrix	55.18	5.76	3.73	13.76	6.21	2.46		11.33	1.57
	4	silicate matrix	48.98	5.4	4.16	14.05	7.11	4.41		13.91	1.99
	5	spinel	60.64	7.92	9.11	0.67	1.50	19.58	0.58		
C	1	pseudobrookite	61.1		6.15	2.43		17.42	12.91		
	2	spinel	61.75	7.07	15.25	0.51	2.04	13.38			
	3	silicate matrix	55.15	2.93	7.07	5.28	2.8	1.58		21.81	3.38
	4	vanadium-rich phase	51.16	4.23	1.86	20.21	9.91	5.33		5.23	2.07

Table IV. Leaching Rate of Roasted Vanadium Slag, Pct

		Oxygen Blowing Time		
Raw Material	MgO Content (Pct)	10 Min	20 Min	30 Min
Industrial Vanadium Slag	4.01	14.63	18.02	18.99
Vanadium Slag with High MgO Content	8.58	23.19	40.38	53.69

D. *Effect of Oxidation Time on the Leaching Rate of Vanadium*

Table IV shows the leaching rates of the roasted vanadium slags. The acid leaching conditions are as follows: liquid-to-solid ratio 5:1, temperature 70 °C, time 30 minutes, pH 0.5 and stirring speed 100 rpm. The leaching rate of roasted vanadium slag with high MgO content is significantly higher than that of industrial vanadium slag. The leaching rate of vanadium of roasted vanadium slag increases obviously with the increase of oxygen blowing time. With the increase of oxygen blowing time from 10 to 30 minutes, the leaching rate of roasted industrial vanadium slag increases from 14.63 to 18.99 pct, while the leaching rate of roasted vanadium slag with high MgO content increases from 23.19 to 53.69 pct.

The XRD pattern of the residue of the vanadium slag with high MgO content oxidized for 30 minutes is shown in Figure 8. The main components of the leaching residue are Fe_2TiO_5, $MgFeAlO_4$ and Fe_2O_3. The diffraction peak of magnesium pyrovanadate $Mg_2V_2O_7$ disappeared, and a weak SiO_2 diffraction peak appeared. The reaction is shown in Eqs. [3], [4].

$$Mg_2V_2O_7 + 3H_2SO_4 = (VO_2)_2SO_4 + 2MgSO_4 + 3H_2O \quad [3]$$

$$MgSiO_3 + H_2SO_4 = SiO_2 + MgSO_4 + H_2O \quad [4]$$

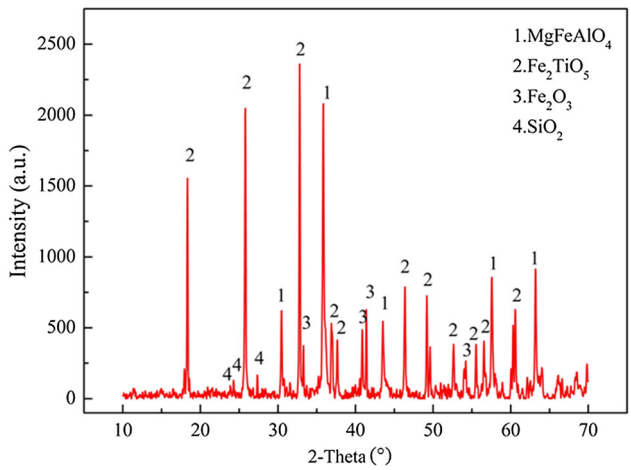

Fig. 8—XRD pattern of the leaching residue of vanadium slag with high MgO content.

E. *Oxidation Mechanism of Vanadium Slag with High MgO Content*

As mentioned above, during the oxidation process, the olivine phase $(Mg, Fe)_2SiO_4$ in the vanadium slag preferentially reacts to form the pyroxene phase $MgSiO_3$, and Mg^{2+} gradually enters into the silicate matrix. Part of Mg^{2+} in the silicate matrix is also involved in the formation of $MgFeAlO_4$, and the generation of $MgFeAlO_4$ brings free SiO_2. The reaction

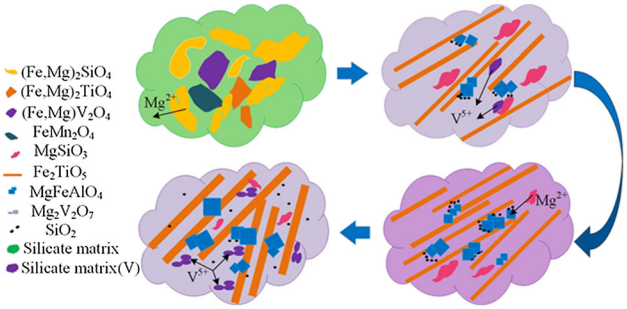

Fig. 9—Oxidation step of vanadium slag with high MgO content.

is shown in Eqs. [1], [2]. The spinel phase of Fe_2TiO_4 at the edge of the spinel phase is oxidized into Fe_2TiO_5. The spinel is broken and disintegrated, and a large amount of vanadium gradually enters into the silicate matrix. With the increase of oxidation time, the slender pseudobrookite Fe_2TiO_5 crystals grow and polymerize into rod-shaped Fe_2TiO_5. The amorphous morphology of the solid solution of magnesium pyrovanadate (Mg, Mn, Ca)$_2V_2O_7$ began to incorporate from the silicate matrix. The reaction is shown in Eqs. [5], [6], [7], [8], [9], [10] and [11]. The oxidation step of vanadium slag with high MgO content is shown in Figure 9.

$$2Fe_2SiO_4 + 2MgO + O_2 = 2MgSiO_3 + 2Fe_2O_3 \quad [5]$$

$$4FeO + O_2 + 2TiO_2 = 2Fe_2TiO_5 \quad [6]$$

$$2Fe_2TiO_4 + O_2 = 2Fe_2TiO_5 \quad [7]$$

$$1/2FeV_2O_4 + MgSiO_3 + 5/8O_2 = 1/2Mg_2V_2O_7 + 1/4Fe_2O_3 + SiO_2 \quad [8]$$

$$MgV_2O_4 + MgSiO_3 + O_2 = Mg_2V_2O_7 + SiO_2 \quad [9]$$

$$1/2FeV_2O_4 + MgO + 5/8O_2 = 1/2Mg_2V_2O_7 + 1/4Fe_2O_3 \quad [10]$$

$$MgV_2O_4 + MgO + O_2 = Mg_2V_2O_7 \quad [11]$$

IV. CONCLUSIONS

This article studied the oxidation mechanism of vanadium slag with the high MgO content at high temperature and drew the following conclusions:

1. The main phases of vanadium slag with high MgO content are spinel phase (Fe, Mg)V_2O_4, (Mg, Fe)$_2$-TiO_4 and olivine phase (Mg, Fe)$_2SiO_4$. Mg is concentrated in the olivine phase and spinel phase, and V is only concentrated in the spinel phase.
2. During the oxidation process, (Mg, Fe)$_2SiO_4$ preferentially reacted into $MgSiO_3$, and then the spinel phase was oxidized into a large amount of strip pseudobrookite Fe_2TiO_5, and vanadium gradually began to disperse in the matrix silicate. Finally, the crystal formed by the reaction grew and polymerized, which made pseudobrookite on the silicate matrix bulky, and the amorphous morphology of the solid solution of magnesium pyrovanadate (Mg, Mn, Ca)$_2V_2O_7$ began to incorporate from the silicate matrix.
3. At 1723 K, the conversion of trivalent vanadium to pentavalent vanadium can be achieved by oxygen blowing roasting with the sensible heat of vanadium slag. The leaching rate of roasted vanadium slag with high MgO content is significantly higher than that of industrial vanadium slag. Oxygen blowing time positively promotes the leaching rate of roasted vanadium slag. With the increase of oxygen blowing time from 10 to 30 minutes, the leaching rate of roasted vanadium slag with high MgO content increases from 23.19 to 53.69 pct.

ACKNOWLEDGMENTS

This work was supported by the National Natural Science Foundation of China (No. 51974047) and Natural Science Foundation of Chongqing, China (No. cstc2020jcyj-msxmX0043).

CONFLICT OF INTEREST The authors declare that they have no conflicts of interest.

REFERENCES

1. W.Z. Mu, T.A. Zhang, Z.H. Dou, G.Z. Lv, and Y. Liu: *Trans. Nonferrous Met. Soc. China*, 2011, vol. 21, pp. 2078–86.
2. R.R. Moskalyk and A. Alfantazi: *Miner. Eng.*, 2003, vol. 16 (9), pp. 793–805.
3. B.V.R. Raja, *Qual. Assur.*, 2007, pp. 19-22.
4. G.B. Sadykhov and I.A. Karyazin: *Russ. Metall.*, 2007, vol. 6, pp. 447–54.
5. L Yu, YC Dong, GZ Ye, and SC Du: *Ironmak. Steelmak.*, 2007, vol. 34, pp. 131–37.
6. G. B. Sadykhov: *Russ. Metall.*, 2008, pp. 449–58.
7. S. Gustafsso and W.W. Zhong: *Int. J. Miner. Process*, 1985, vol. 15, pp. 103–15.
8. J. Diao, W. Zhou, P. Gu, Z.Q. Ke, and B. Xie: *CrystEngComm*, 2016, vol. 18, pp. 6272–81.
9. HY Gao, T Jiang, YZ Xu, J Wen, and XX Xue: *Powder Technol.*, 2018, vol. 340, pp. 20–527.
10. G. Zhang, D.Q. Luo, D.M. Deng, C.H. Lv, L. Li, and B. Li: *J. Alloys Compd.*, 2018, vol. 742, pp. 504–11.
11. X.S. Li and B. Xie: 2012*Int. J. Miner. Metall. Mater.*, 2012, vol. 19, pp. 595–601.
12. G.B. Sadykhov: *Russ. Metall.*, 2008, vol. 2008, pp. 449–58.
13. A. Mahdavian, A. Shafyei, E.K. Alamdari, and D.F. Haghshenas: *Int. J. Iron Steel Soc. Iran*, 2006, vol. 3, pp. 17–21.
14. Y.M. Zhang, S.X. Bao, T. Liu, T.J. Chen, and J. Huang: *Hydrometallurgy*, 2011, vol. 109, pp. 116–24.

15. L. Jia, Y. Zhang, L. Tao, H. Jing, and S. Bao: *J. Clean. Prod.*, 2014, vol. 84, pp. 598–605.
16. JW Wen, PG Ning, HB Cao, ZHI Sun, and Y Zhang: *J. Clean. Prod.*, 2018, vol. 205, pp. 728–37.
17. M. Aarabi-Karasgani, F. Rashchi, N. Mostoufi, and E. Vahidi: *Hydrometallurgy*, 2010, vol. 102, pp. 14–21.
18. Z Yang, HY Li, XC Yin, ZM Yan, XM Yan, and B Yie: *Int. J. Miner. Process*, 2014, vol. 133, pp. 105–11.
19. H.Y. Li, C. J. Wang, Y. H. Yuan, Y. Guo, J. Diao, and B. Xie: *J. Clean. Prod.*, 2020, vol. 260.
20. W.C. Song, H. Li, F.X. Zhu, K. Li, and Q. Zheng: *Trans. Nonferrous Met. Soc. China*, 2014, vol. 24, pp. 2686–93.
21. W.C. Song, H. Li, Y.N. Wang, F. Zhu, K. Li, and Q. Zheng: *Chin. J. Rare Met.*, 2014, vol. 38, pp. 874–79.
22. L. Liang, Y.W. Bao, Q.X. Yang, Y.H. Chen, G.Q. Liu, F.L. Han, J. Wei, F. Engstrom, and J.Y. Deng: *Steel Res. Int.*, 2017, vol. 88 (11), art. no. e201700066.
23. S.C. Panigrahy, P. Verstraeten, and J. Dilewijns: *Metall. Mater. Trans. B*, 1984, vol. 15B, pp. 23–32.
24. P. Xue, D.F. He, A.J. Xu, Z.X. Gu, Q.X. Yang, F. Engström, and B. Björkman: *J. Alloys Compd.*, 2017, vol. 72, pp. 640–48.
25. W. Zhao, M.S. Chu, C. Feng, H.T. Wang, Z.G. Liu, J. Tang, and and W.P. Wang: *Ironmak. Steelmak.*, 2020, vol. 47 (4), pp. 388–97.